Title	Elastic Scattering of 100- and 200-keV Positrons by Selenium and Bismuth
Author(s)	Kobayashi, Takayuki; Shimizu, Sakae
Citation	Bulletin of the Institute for Chemical Research, Kyoto University (1973), 50(5): 488-498
Issue Date	1973-02-28
URL	http://hdl.handle.net/2433/76455
Right	
Type	Departmental Bulletin Paper
Textversion	publisher

Bull. Inst. Chem. Res., Kyoto Univ., Vol. 50, No. 5, 1972

Elastic Scattering of 100- and 200-keV Positrons by Selenium and Bismuth

Takayuki KOBAYASHI and Sakae SHIMIZU*

Received July 24, 1972

The differential cross sections for elastic scattering of positrons in $_{34}$Se and $_{83}$Bi targets were measured at 30°, 40°, 60° and 85° for energies of 100 and 200 keV. Positron beams of these energies were obtained by the use of a sector-type double-focusing β-ray spectrometer mounted with a ^{22}Na source. Scattered positrons were measured by semiconductor (silicon) detectors in a scattering chamber. The experimental results were compared with the theoretical values calculated by the Mott phase-shift method. Though the experimental cross sections were, on the whole, in agreement with the theoretical values, the experimental cross sections tend to be lower than the theoretical ones, especially in the case of 100-keV positron scattering in Bi targets. This phenomenon was considered to be due to the effect of local distortion of the electron cloud by the incident particle.

I. INTRODUCTION

Many works have so far been attempted on elastic scattering of electrons theoretically and/or experimentally.[1~6] Most of the experimental works show that the phase-shift theory presented by Mott[1,2] gives the correct cross section of elastic scattering of electrons. However, Rester and Rainwater's work,[6] one of the most reliable experiments for Al, shows that at energies of 100 and 200 keV their measured cross sections are apparently lower than those calculated by Doggett and Spencer[2] for pure Coulomb field. It cannot be supposed that this discrepancy occured owing only to the screening effect of atomic electrons. It is interesting to investigate whether the discrepancy between the experimental and theoretical cross sections would be observed for elastic scattering of positrons at energies of 100 and 200 keV.

The elastic scattering of positrons was first discussed by Massey[7] by changing Z to $-Z$ in the Mott phase-shift formula.[1,2] Though many measurements have been made on elastic scattering of electrons, a few works have been done on scattering of positrons. This is no doubt due to a lack of a suitable source of positrons. The first experiment on positron scattering was attempted by Fowler and Oppenheimer.[8] They measured only a small number of scattering events with a cloud chamber, and could not check the theory quantitatively. Lipkin and White[9] first employed a counter to investigate 0.7-MeV positron scattering in a Pt foil at 58°. Reliable measurements were done by Ellis and Henderson[10] with Al, Ag and Au foils for energies of 0.7 and 1.4 MeV at angles of 22.8°, 34.5° and 47.5°. They found a good agreement with the theory. The absolute cross section was first obtained by Bowness and Cusack[11] with

* 小林 隆幸, 清水 栄: Laboratory of Nuclear Radiation, Institute for Chemical Research, Kyoto University, Kyoto.

a cloud chamber for Ar at an energy of 300 keV at angles larger than 30°. No experimental work using counters with good statistics has so far been reported on scattering of positrons for energies lower than 300 keV.

The present paper reports the experimental determination of the cross sections for elastic scattering of positrons for energies of 100 and 200 keV in Se and Bi foils with an aim to investigate whether the discrepancy between the experimental and theoretical cross sections would be observed or not as in the scattering of electrons measured by Rester and Rainwater.[6]

II. THEORETICAL CALCULATIONS OF THE CROSS SECTION

In order to compare with the experimental results, theoretical calculations of the elastic scattering cross section of positrons have been performed numerically by Mott's exact phase-shift method.[1,2] In this section, r denotes the distance between the center of the potential and the scattered particle and θ the scattering angle. Energies are represented in units of mc^2, momenta in mc and lenghts in the Compton wave length of an electron. Here m and c are the rest mass of an electron and the speed of light in vacuum, respectively.

Mott obtained the elastic scattering cross section in the exact form as

$$\frac{d\sigma}{d\Omega}=|f(\theta)|^2+|g(\theta)|^2\,, \tag{1}$$

where

$$f(\theta)=\frac{1}{2ip}\sum_{l=0}^{\infty}[(l+1)\{\exp(2i\delta_l)-1\}+l\{\exp(2i\delta_{-l-1})-1\}]P_l(\cos\theta), \tag{2}$$

$$g(\theta)=\frac{1}{2ip}\sum_{l=1}^{\infty}[\exp(2i\delta_{-l-1})-\exp(2i\delta_l)]P_l^1(\cos\theta). \tag{3}$$

In Eqs. (2) and (3), p is the momentum of the incident particle, $P_l(\cos\theta)$ and $P_l^1(\cos\theta)$ are the Legendre function and the associated Legendre function, respectively, and δ_l is the phase shift. Lin *et al.*[12] derived an equation for the phase shift as

$$\frac{d\eta_l}{d\xi}=-\left[\frac{l(l+1)}{\xi^2}+\frac{U_l}{p^2}\right]\sin^2(\xi+\eta_l), \tag{4}$$

when $\xi(=pr)\to\infty$, $\eta_l\to\left(\delta_l-\frac{1}{2}l\pi\right)$. In this equation

$$U_l=2WV-V^2-\frac{l+1}{\xi}p^2\frac{D'}{D}+\frac{3}{4}p^2\frac{D'^2}{D^2}-\frac{1}{2}p^2\frac{D''}{D}\,, \tag{5}$$

where $D=W-V+1$, $D'=dD/d\xi$, $D''=d^2D/d\xi^2$, and W and V denote the total energy of the incident particle and a potential, respectively. They obtained the initial value of η_l from the power series expansion of η_l and U_l near the origin provided the wave function G_l, the solution of the Dirac equation, vanishes there. However, in the present calculations the initial value is obtained by the other procedure; from Eqs. (3) and (4)′ in the paper of Lin *et al.* as

$$\eta_l=\tan^{-1}\left(G_l\Big/\frac{dG_l}{d\xi}\right)-\xi\,, \tag{6}$$

except at $\xi=0$. The wave function G_l near the origin is represented in a form of the

power series expansion of ξ.

When the series for f and g, Eqs. (2) and (3), are summed by the use of phase-shifts thus obtained, the "reduced series" method described in the paper of Lin[13] can be applied to improve the convergence.

III. APPARATUS

A. Positron Monochrometer

In order to prepare a monoenergetic positron beam using a β^+-decay ^{22}Na source, a sector-type double-focusing β-ray spectrometer with a reference radius of 11 cm was constructed. This is composed of two semi-circular iron pole pieces of 24 cm in diameter and coils. An aim of the design was to supply a considerable intense parallel beam with a good momentum resolution and to allow enough space around the focusing point for a scattering chamber, in which relative position of a target foil and a detector could be changed. The momentum resolution and transmission achieved by this monochrometer were 1.43 % and 0.93 %, respectively. In the present measurement, however, by the needs for the beam collimation and arrangements of the scatterer foil and the detector, only 0.04 % or 0.05 % of positrons from the source was used with the momentum resolution of 2.18 % or 3.2 %, respectively.

An evaporation residuum of the $^{22}NaCl$ solution of about 3 mCi was mounted in the monochrometer as a positron source. This nuclide was chosen because of its long life and the peak of the β^+ spectrum being close to the energies to be studied in the present work.

B. Scattering Chamber

The experimental arrangement is shown in Fig. 1. The scattering chamber is connected to the exit of the vacuum chamber of the monochrometer by a flexible bellows, by which the relative position of both chambers can be adjusted so that positrons would impinge on the scatterer foil at right angle. The main body of the scattering chamber, made of 2-cm thick Lucite plates, has a round cover plate with a turning device for the detector.

The collimator assembly before the scattering foil is rather complicated as shown in Fig. 1. The diameter of the holes of two 1-mm thick aluminum diaphragms (D_1 and D_2) is 4.1 or 2.4 mm when distance between both diaphragms is set to be 11 or 26 mm, respectively. Another aluminum baffle (A) of 1-mm thickness is also used between D_1 and D_2 in order to stop positrons with energies differ from the designated energy. An iron plate (F) with a hole of 8.2 mm in diameter is inserted just in front of the central baffle A to reduce leakage of the magnetic flux in the vicinity of the focusing point. The very small existing leakage flux was proved to be no disturbance for the present work. To reduce background due to the annihilation rays of positrons, lead plate (L) are arranged as shown in the figure. The diameter of the focused beam at the target foil was found to be about 5 or 3 mm by permitting the beam to pass through a piece of x-ray film according to two different arrangements of D_1 and D_2.

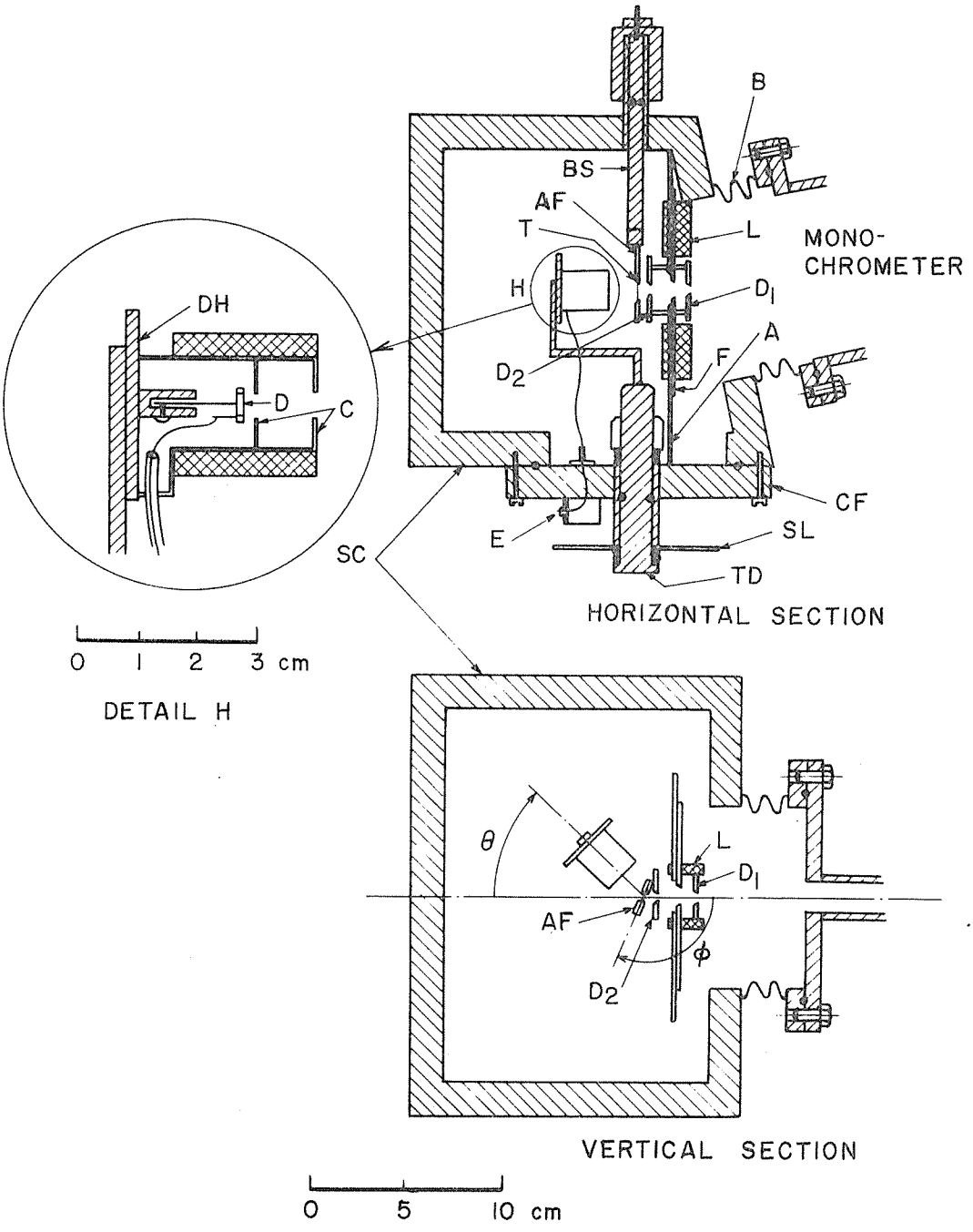

Fig. 1. Experimental arrangement. SC: scattering chamber, B: bellows, L: lead shield, D_1 and D_2: aluminum diaphragms, A: aluminum baffle, F: iron plate, CF: round cover plate, TD: turning device, SL: scale, E: electric connector, AF: aluminum frame, T: scatterer, BS: brass shaft, C: collimator, D: detector, DH: detector holder, θ: scattering angle, ϕ: angle of the scatterer surface against the incident positron beam.

A thin foil of the target material is mounted on a rectangular aluminum frame supported by a brass shaft, which can be adjusted from outside the chamber. Two elements $_{34}$Se and $_{83}$Bi have been chosen as the target material, by taking account of easy preparation of very thin foils with large area by the evaporation technique. These elements were evaporated on Formvar backings of about 2 $\mu g/cm^2$ thickness streched tightly over a 10-mm diameter hole of an aluminum plate. The thickness of the foil was determined with an error less than 5 % by a quartz crystal microbalance monitor, model DTM-3 of Sloan Instruments Corporation. The thicknesses of the target foils used are given in Table 1.

Table 1. Thickness of the Prepared Target Foils.

$_{34}$Se		$_{83}$Bi	
Foil No.	Thickness ($\mu g/cm^2$)	Foil No.	Thickness ($\mu g/cm^2$)
Se-1	21.5± 1.1	Bi-1	10.9±0.6
Se-2	50.4± 2.4	Bi-2	21.8±1.1
Se-3	100 ± 5	Bi-3	48.2±2.5
Se-4	203 ±10	Bi-4	98.9±5.0

In the present work, two lithium-drifted silicon detectors (called Si(Li)-1 and Si(Li)-2) and a surface barrier silicon detector (SiD-3) were used. The detectors Si(Li)-2 and SiD-3 were used for measurements of the scattered positrons of 200 and 100 keV, respectively, while Si(Li)-1 was for counting of incident positrons of these energies on the traget foils. The characteristics of the detectors are given in Table 2.

Table 2. Characteristic of the Silicon Detectors.

Name	Type	Thickness of the depletion layer (mm)	Sensitive area (mm^2)	Energy resolution[a] (keV)
Si(Li)-1	Lithium-drifted	1.0	38	20.0
Si(Li)-2	Lithium-drifted	1.0	5	18.5
SiD-3	Surface barrier	0.12	8	10.5

[a] fwhm at room temperature.

Depleted layers of Si(Li)-1 and -2 are thicker than the range of 200-keV positrons in silicon and that of SiD-3 is thicker than the range of 100-keV positrons. The detector Si(Li)-2 or SiD-3 was mounted on the detector holder at a distance of 27 mm from the target in the scattering chamber. When the number of positrons impinging on the target was measured, another detector holder for Si(Li)-1 with larger aperture and without collimator was used. The amplifier for the detector is a low-noise system similar to that of ORTEC 101-201 type.

IV. EXPERIMENTAL PROCEDURE

The number of positrons impinging on the target foil was first measured by the

detector Si(Li)-1 placed at the focusing point, and then the spectra of scattered positrons from the target were observed at selected angles by the detector Si(Li)-2 for 200-keV incident positrons or by SiD-3 for 100-keV incident positrons. To estimate the background under the same experimental condition the target foil was replaced by a Formvar foil. Each experimental run for scattering positrons was followed by a background run with only the Formvar foil.

The spectrum of the incident monoenergetic positrons observed with the solid detector is composed of two parts, a peak of Gaussian distribution and a low-energy tail. This tail is mainly due to positrons backscattered out from the detector surface before losing their total kinetic energy. However, it is well known that for the silicon

Table 3. Experimental Conditions for 100-keV Measurements.

	$\theta^{a)}$ (deg.)	Foil No.	$\phi^{b)}$ (deg.)	$l_a{}^{c)}$ (mm)	$d_a{}^{d)}$ (mm dia.)	$G^{e)}$	$E^{f)}$ (%)
$_{34}$Se	30	Se-1	90	26	2.4	1.037	5.0
	40	Se-1	90	11	4.1	1.079	2.8
	60	Se-2	135	11	4.1	1.037	3.9
	85	Se-3	135	11	4.1	1.017	3.8
$_{83}$Bi	30	Bi-1	90	26	2.4	1.037	5.0
	40	Bi-1	90	11	4.1	1.079	2.9
	60	Bi-2	135	11	4.1	1.037	3.8
	85	Bi-3	135	11	4.1	1.017	4.4

a) Scattering angle.
b) Angle of the target against the incident positron beam.
c) Distance between the diaphragms D_1 and D_2.
d) Aperture of the diaphragms.
e) Finite geometry correction factor.
f) Fractional error by multiple scattering.

Table 4. Experimental Conditions for 200-keV Measurements.

	$\theta^{a)}$ (deg.)	Foli No.	$\phi^{b)}$ (deg.)	$l_a{}^{c)}$ (mm)	$d_a{}^{d)}$ (mm dia.)	$G^{e)}$	$F^{f)}$ (%)
$_{34}$Se	30	Se-2	90	26	2.4	1.035	3.3
	40	Se-3	90	11	4.1	1.078	3.7
	60	Se-3	135	11	4.1	1.036	2.3
	85	Se-4	135	11	4.1	1.017	2.2
$_{83}$Bi	30	Bi-2	90	26	2.4	1.035	3.2
	40	Bi-3	90	11	4.1	1.078	4.0
	60	Bi-3	135	11	4.1	1.036	2.5
	85	Bi-4	135	11	4.1	1.017	2.4

a) Scattering angle.
b) Angle of the target against the incident positron beam.
c) Distance between the diaphragms D_1 and D_2.
d) Aperture of the diaphragms.
e) Finite geometry correction factor.
f) Fractional error by multiple scattering.

detectors thicker than the range of incident particles have the same peak-to-total ratio, as shown in the work by Berger *et al.*[14] This fact was also verified within the statistical errors for the detectors used in this work. For this reason, to estimate the elastic scattering cross section the ratio of areas under the peaks in the pulse-height spectra was measured for incident and scattered positrons.

The scattering measurements were performed at 30°, 40°, 60° and 85° with both Se and Bi target foils. The measurement with the target foil at a selected angle was repeated to obtain the desired counting statistics. In Tables 3 and 4 are given the experimental conditions, chosen in the present work so as to make the experimental corrections permissibly small. The effective solid angle Ω subtended by the detector to the center of the target foil was determined exactly by comparing the counting rates of conversion electrons from a ^{137}Cs point source and/or α particles from an ^{241}Am point source mounted on the center of the foil with counting rates observed by an appropriate standard geometry having the same source and a known solid angle. The numerical values thus determined are $\Omega=(7.34\pm0.15)\times10^{-3}$ sr for the Si(Li)-2 detector for 200-keV positrons and $\Omega=(1.35\pm0.03)\times10^{-2}$ sr for the SiD-3 detector for 100-keV positrons. As discussed later, the corrections were made for multiple scattering of positrons in the target foil, the finite geometrical sizes of the focusing image and the detector, and the finite angular spread of the positron beam.

The good stability of the whole system was crucial to the success of the experiment, because the long-term measurements were required. The stability of the gain of the detector and the electronic system was checked before and after each experimental run. The variation in the exciting current of the magnet of the positron monochrometer was achieved less than $\pm10^{-2}$ %.

V. CORRECTIONS

A. Correction for Finite Geometry

In order to estimate the effects of finite angular spread of the incident beam and finite sizes of the focusing image on the target and of the detector, the formula of Willmes[15] was referred. The measured counting rate of the scattered particles C is given by

$$C=C_0G, \tag{7}$$

where C_0 is the counting rate under the condition ignoring the finite geometry effects and G the finite geometry correction factor. When r_1 and r_2 are the radii of the hole of the diaphragm D_1 (and D_2) and the detector, respectively, and the beam spot on the target plane is an ellipse with a long axis $2a$ and a short one $2b$, G can be expressed by

$$G=A_0+\frac{2A_1}{1-\cos\theta}+\frac{6A_2}{(1-\cos\theta)^2}, \tag{8}$$

where A_0, A_1 and A_2 are given by

$$A_0=1-\frac{3}{32R_0^2}[a^2\{1-3\cos^2(\theta-\phi)\}+b^2+2r_2^2], \tag{9a}$$

$$A_1=\frac{1}{16}\left[a^2h_1+b^2h_2-\cos\theta\left\{\left(\frac{r_1}{D}\right)^2+\left(\frac{r_2}{R_0}\right)^2\right\}\right], \tag{9b}$$

$$A_2=\frac{1}{16}\left[a^2h_3+\frac{1}{2}\left\{\left(\frac{r_1}{D}\right)^2\cos\theta+\left(\frac{r_2}{R_0}\right)^2\sin^2\theta\right\}\right]. \tag{9c}$$

Here, ϕ and θ are defined in Fig. 1, D and R_0 are the distances between the diaphragm D_1 and target, and between the target and detector, respectively, and h_1, h_2 and h_3 are defined as

$$h_1=\frac{b_1}{D^2}+\frac{b_2}{R_0^2}+\frac{b_3}{DR_0},$$

$$b_1=-0.5\cos\theta(1-3\cos^2\phi)-\cos(\theta-\phi)\cos\phi,$$

$$b_2=-3\cos(\theta-\phi)\cos\phi+3.5\cos\theta\cos^2(\theta-\phi)-0.5\cos\theta,$$

$$b_3=-3\cos\theta\cos(\theta-\phi)\cos\phi+3\cos^2(\theta-\phi)-\sin^2\phi,$$

$$h_2=-\frac{\cos\theta}{2D^2}-\frac{\cos\theta}{2R_0^2}-\frac{1}{DR_0},$$

$$h_3=\frac{C_1}{D^2}+\frac{C_2}{R_0^2}+\frac{C_3}{DR_0},$$

$$C_1=0.5\cos^2(\theta-\phi)+0.5\cos^2\theta\cos^2\phi-\cos\phi\cos(\theta-\phi)\cos\theta,$$

$$C_2=0.5\cos^2\phi+0.5\cos^2\theta\cos^2(\theta-\phi)-\cos\theta\cos(\theta-\phi)\cos\phi,$$

$$C_3=-\cos(\theta-\phi)\cos\phi+\cos\theta\cos^2(\theta-\phi)+\cos\theta\cos^2\phi-\cos^2\theta\cos(\theta-\phi)\cos\phi.$$

The numerical values of G in Eq. (7) thus estimated and used are given in Tables 3 and 4.

B. Correction for Multiple Scattering

In order to estimate the correction for multiple scattering of positrons in the traget foil, the fractional error by this effect derived by Chase and Cox[4] was applied. They obtained the expression

$$\langle\varepsilon^2\rangle\left(\mathrm{cosec}^2\frac{\theta}{2}-\frac{1}{2}\right). \tag{10}$$

Here, $\langle\varepsilon^2\rangle$ is the mean square deflection of the scattered positrons. The square angle $\langle\varepsilon^2\rangle$ can be calculated with a sufficient accuracy using the expression given by Groetzinger *et al.*[16] as

$$\langle\varepsilon^2\rangle=\frac{4\pi Nte^4Z(Z+1)}{(pv)^2}S. \tag{11}$$

Here, e, p and v are the charge, momentum and velocity of the particle, respectively, N the number of atoms in the target foil per unit volume, Z the atomic number of the target atom, t the foil thickness, and S a very slow varying function of Z and p. The value of $S=2.3$, measured by Kinzinger and Bothe[5] for a case of 245-keV electron in aluminum, was adopted in the present work, since S can be treated as a constant for the practical purpose. The corrections thus estimated in the present experiment are less than 5% for all scattering angles, as listed in Tables 3 and 4.

VI. RESULTS AND DISCUSSION

In Table 5 and Figs. 2 and 3, the experimental cross sections normalized to the Mott cross section are shown. Experimental results shown were obtained by applying

Table 5. Experimental Cross Sections Normalized to the Mott Cross Section.

$\theta^{a)}$ (deg.)	$\frac{d\sigma}{d\Omega}\Big\|_{exp}$ (b/sr)	$\frac{d\sigma}{d\Omega}\Big\|_{exp}/\frac{d\sigma}{d\Omega}\Big\|_{Mott}$	$\frac{d\sigma}{d\Omega}\Big\|_{exp}$ (b/sr)	$\frac{d\sigma}{d\Omega}\Big\|_{exp}/\frac{d\sigma}{d\Omega}\Big\|_{Mott}$
	100 keV		200 keV	
		Se		
30	$(3.35\pm0.19)\times10^{4}$	0.957 ± 0.054	$(9.61\pm0.61)\times10^{3}$	0.983 ± 0.062
40	$(1.10\pm0.07)\times10^{4}$	0.957 ± 0.061	$(2.90\pm0.18)\times10^{3}$	0.964 ± 0.060
60	$(2.56\pm0.14)\times10^{3}$	1.067 ± 0.058	$(6.82\pm0.44)\times10^{2}$	1.057 ± 0.068
85	$(6.81\pm0.37)\times10^{2}$	0.973 ± 0.053	$(1.81\pm0.16)\times10^{2}$	1.023 ± 0.090
		Bi		
30	$(1.64\pm0.10)\times10^{5}$	0.976 ± 0.060	$(5.41\pm0.33)\times10^{4}$	1.055 ± 0.064
40	$(5.05\pm0.33)\times10^{4}$	0.948 ± 0.062	$(1.60\pm0.08)\times10^{4}$	0.936 ± 0.049
60	$(1.18\pm0.07)\times10^{4}$	0.967 ± 0.057	$(3.46\pm0.20)\times10^{3}$	0.975 ± 0.056
85	$(3.72\pm0.20)\times10^{3}$	0.956 ± 0.052	$(9.36\pm0.67)\times10^{2}$	0.975 ± 0.070

a) Scattering angle.

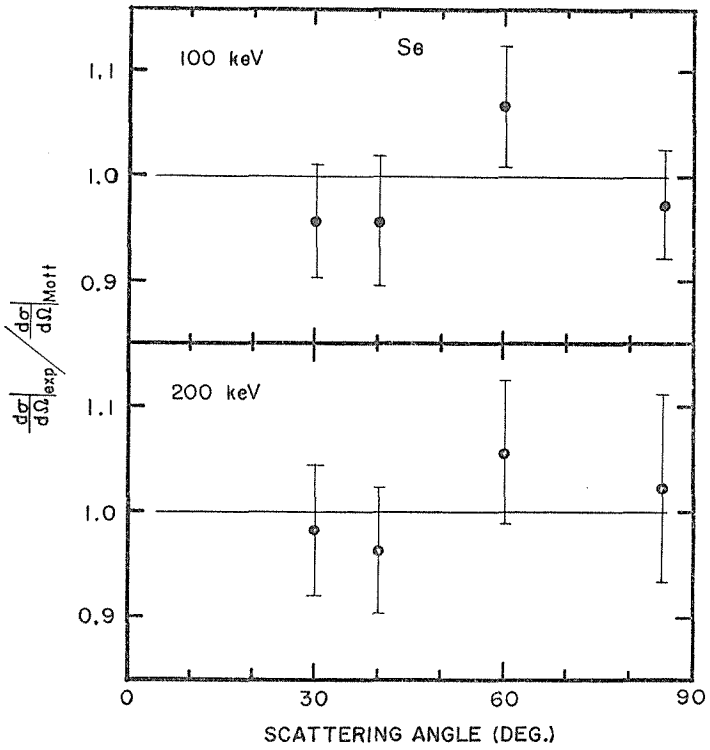

Fig. 2. Experimental cross sections of elastic scattering of 100- and 200-keV positrons by $_{34}$Se. The experimental cross sections $d\sigma/d\Omega|_{exp}$ are normalized to the Moot cross section $d\sigma/d\Omega|_{Mott}$.

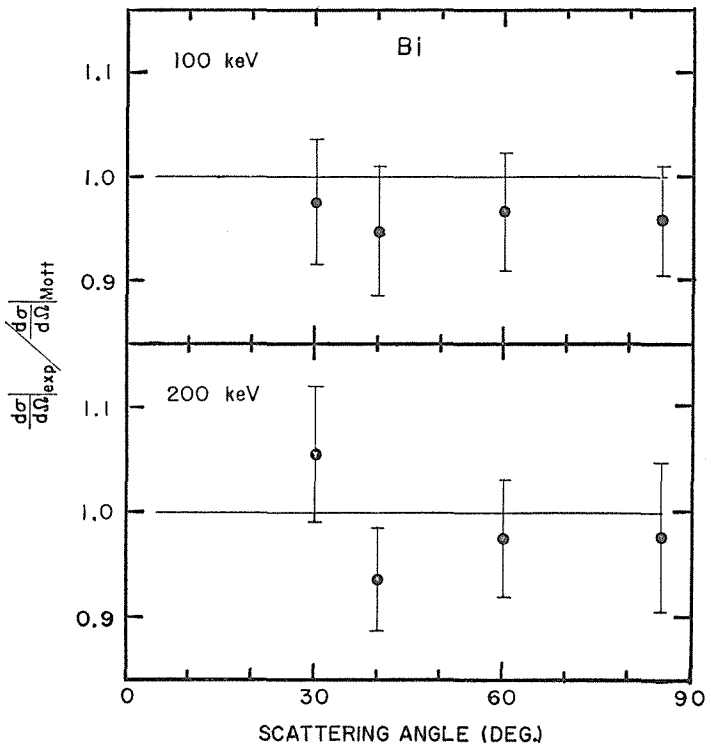

Fig. 3. Experimental cross sections of elastic scattering of 100- and 200-keV positrons by $_{83}$Bi. The experimental cross sections $d\sigma/d\Omega|_{exp}$ are normalized to the Mott cross section $d\sigma/d\Omega|_{Mott}$.

the corrections discussed in the preceding section to the measured values. The experimental error shown in the table and figures is mainly ascribed to an uncertainty in the determination of the target thickness. The Mott cross section was calculated by the use of the Hartree-Byatt screened potential.[17]

The experimental results are, on the whole, in agreement with the theory, and apparement discrepancy between the experimental and theoretical cross sections cannot be recognized. However, the experimental cross sections tend to be lower than the theoretical onès, especially in the case of 100-keV positron scattering by Bi targets.

When the energy of the incident particle is low, lower than several hundred eV, the polarization of the potential caused by the distortion of the target atom in the electron field of the incident particle plays an important role in the scattering process. This is not the case of the present experiment. When the energy is higher and near the binding energy of the inner shell electrons of the atom as in the present case, it is possible that the electron cloud of the atom is deformed partly *i.e.*, the cloud undergoes a local disturbance. This is because the part of the electron cloud to which the outer shell electrons contribute cannot make rapid distortion by the incident particle. The above deformation of the electron cloud may be possible to affect the value of the cross section.

In order to investigate, in more detail, whether the discrepancy between the ex-

perimental and theoretical cross sections would be observed, it would be favorable to measure relative cross sections by the use of the same target foil at various scattering angles. This is because the main source of the experimental error is an uncertainty in the target thickness. In the present experiment, since the positron beam with satisfactory intensity was not available, the scattered positrons could not be measured at 85° with similar good statistics using the same foil as at 30°. More accurate scattering cross sections of positrons at smaller angles are hoped to be measured by the use of a stronger positron beam.

ACKNOWLEDGMENTS

The authors wish to thank Professor T. Naiki of Kyoto Technical University for his kind help in preparation of the scattering foils. They are also indebted to Y. Nakayama, R. Kakano and Y. Isozumi for assistances in the experiment. This work was supported by the Research Grant from the Ministry of Education.

REFERENCES

(1) N. F. Mott, *Proc. Roy. Soc. A*, **124**, 425 (1929) ; *ibid.*, **135**, 429 (1932).
(2) J. A. Doggett and L. V. Spencer, *Phys. Rev.*, **103**, 1597 (1956).
(3) E. Zeitler and H. Olsen, *Phys. Rev.*, **136**, A1546 (1964) ; *Z. Naturforsch.*, **21a**, 1321 (1966).
(4) C. T. Chase and R. T. Cox, *Phys. Rev.*, **58**, 243 (1940).
(5) E. Kinzinger and W. Bothe, *Z. Naturforsch.*, **7a**, 390 (1952).
(6) D. H. Rester and W. J. Rainwater, Jr., *Phys. Rev.*, **140**, A165 (1965).
(7) H. S. W. Massey, *Proc. Roy. Soc. A*, **181**, 14 (1942).
(8) W. A. Fowler and J. Oppenheimer, *Phys. Rev.*, **54**, 320 (1938).
(9) H. J. Lipkin and M. G. White, *Phys. Rev.*, **79**, 892 (1950).
(10) J. Ellis and C. Henderson, *Proc. Roy. Soc. A*, **229**, 260 (1955).
(11) C. Bowness and N. Cusack, *Phil. Mag.*, **2**, 196 (1957).
(12) S. R. Lin, N. Sherman and J. K. Percus, *Nucl. Phys.*, **45**, 492 (1963).
(13) S. R. Lin, *Phys. Rev.*, **133**, A965 (1964).
(14) M. J. Berger, S. M. Seltzer, S. E. Chappell, J. C. Humphreys and J. W. Motz, *Nucl. Instr. Meth.* **69**, 181 (1969).
(15) H. Willmes, *Nucl. Instr. Meth.*, **41**, 122 (1966).
(16) G. Groetzinger, M. J. Berger and F. L. Ribe, *Phys. Rev.*, **77**, 584 (1950).
(17) W. J. Byatt, *Phys. Rev.*, **104**, 1298 (1956).